ISBN: 978-3-95450-194-6 doi:10.18429/JACoW-LINAC2018-TUPO113

BEAM DYNAMICS STUDIES THROUGH DIELECTRIC THZ ACCELERATING STRUCTURES

R. Apsimon*, G. Burt, , A. Healy, S. Jamison, Lancaster University, Bailrigg, UK
A. Latina, CERN, Geneva, Switzerland
R. B. Appleby, E. Smith, University of Manchester, UK

Abstract

As conventional RF accelerating schemes approach the physical limit of accelerating gradient, the accelerator community is increasingly looking at novel accelerating techniques to overcome these limitations. Moving from the RF to the THz frequency range, higher acceleration gradients of high energy beams can be achieved in compact structures. Beam dynamics studies are crucial as part of the design of novel accelerating structures to maximise the output beam current as well as the accelerating gradient. In this paper we present beam dynamics simulations through dielectric lined waveguide structures using novel techniques to simulate broadband signals for particle tracking studies in RF-Track. The beam parameters through the structure are optimised and we study the dynamics of general broadband accelerating structures.

INTRODUCTION

As conventional RF accelerating schemes approach the physical limit of accelerating gradient, the accelerator community is increasingly looking at novel accelerating techniques in the THz regime to overcome these limitations. Dielectric lined waveguides (DLWs) (Figure 1)are one such accelerating technique, favoured for its ability to produce high field gradients as well as its ease of fabrication.

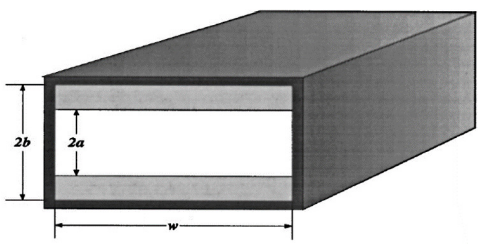

Figure 1: Diagram of a dielectric lined waveguide [1].

Due to the relative simplicity of the physical system for a DLW, a full analytical solution for the electromagnetic fields can be obtained [1]. In this paper, we only consider the LSM_{11} accelerating mode. LSM modes are equivalent to TM modes in a waveguide without any dielectric, but the LSM mode couples to the TM modes in both the vacuum and dielectric regions. If we define a as the half-height of the vacuum region, b as the half-height of the waveguide and w as the full width of the waveguide, as shown in Figure 1, then the dispersion relation for the LSM_{mn} mode is given as

$$k_{mn}^{(1)} \sin\left[k_{mn}^{(1)}(b-a)\right] \sin k_{mn}^{(0)} a - \varepsilon_r k_{mn}^{(1)} \cos\left[k_{mn}^{(1)}(b-a)\right] \cos k_{mn}^{(0)} a = 0 \quad , \tag{1}$$

where

$$k_{mn}^{(0)} = \sqrt{\left(\frac{\omega}{c}\right)^2 - \left(\frac{m\pi}{w}\right)^2 - \beta_{mn}^2}$$
$$k_{mn}^{(1)} = \sqrt{\varepsilon_r \left(\frac{\omega}{c}\right)^2 - \left(\frac{m\pi}{w}\right)^2 - \beta_{mn}^2} \quad . \tag{2}$$

This dispersion relation is a transcendental equation that needs to be evaluated numerically (Figure 2a), but provides a functional relationship between ω and β_{mn}, from which we can obtain the phase velocity, $v_p = \frac{\omega}{\beta_{mn}}$, and group velocity, $v_g = \frac{d\omega}{d\beta_{mn}}$ (Figure 2b). The electric and magnetic fields in the frequency domain within the vacuum region of the DLW respectively are given as

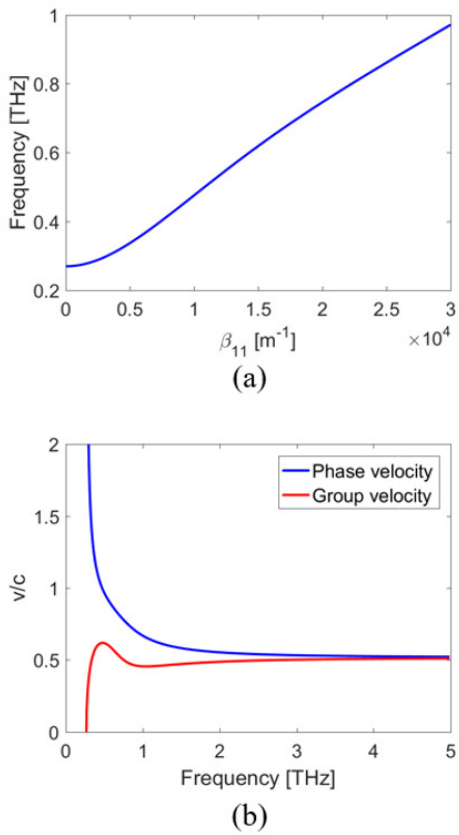

Figure 2: Dispersion relation (a) and phase (blue) and group (red) velocity (b) for a DLW for the LSM_{11} mode with a = 250 µm, b = 300 µm and w = 1200 µm.

* r.apsimon@lancaster.ac.uk

ISBN: 978-3-95450-194-6 doi:10.18429/JACoW-LINAC2018-TUPO113

$$\begin{pmatrix}\mathcal{E}_x\\ \mathcal{E}_y\\ \mathcal{E}_z\end{pmatrix} = Ae^{-j\beta_{mn}z}\begin{pmatrix}\frac{m\pi}{w}k_{mn}^{(0)}\cos\left[\frac{m\pi}{w}\left(x+\frac{w}{2}\right)\right]\cos k_{mn}^{(0)}y\\ \left[\left(\frac{m\pi}{w}\right)^2+\beta_{mn}^2\right]\sin\left[\frac{m\pi}{w}\left(x+\frac{w}{2}\right)\right]\sin k_{mn}^{(0)}y\\ -j\beta_{mn}k_{mn}^{(0)}\sin\left[\frac{m\pi}{w}\left(x+\frac{w}{2}\right)\right]\cos k_{mn}^{(0)}y\end{pmatrix}.$$

$$\begin{pmatrix}\mathcal{H}_x\\ \mathcal{H}_y\\ \mathcal{H}_z\end{pmatrix} = Ae^{-j\beta_{mn}z}\begin{pmatrix}-\omega\varepsilon_0\beta_{mn}\sin\left[\frac{m\pi}{w}\left(x+\frac{w}{2}\right)\right]\sin k_{mn}^{(0)}y\\ 0\\ j\omega\varepsilon_0\frac{m\pi}{w}\cos\left[\frac{m\pi}{w}\left(x+\frac{w}{2}\right)\right]\sin k_{mn}^{(0)}y\end{pmatrix} \quad (3)$$

The ratio of field amplitude in the vacuum (A) and dielectric (B) is dependent on the dispersion relation in Eq. 1 and give as

$$\frac{A}{B} = r_{vd} = \frac{\varepsilon_r\cos\left[k_{mn}^{(1)}(b-a)\right]}{\sin k_{mn}^{(0)}a}. \quad (4)$$

In this paper, we will take this analytical description of a DLW and use it to develop a model for the THz fields due to a broadband input pulse. Furthermore we will develop a technique for tracking a particle beam through such a field. Finally we shall show some preliminary results of such a tracking technique.

BROADBAND THZ PULSES

An infinite duration, pure sinusoidal signal has a single frequency component and therefore has zero bandwidth. As the pulse duration decreases, the bandwidth increases. The advantage of using a broadband pulse to accelerate a particle bunch is that all the power is concentrated into a short duration pulse, resulting in higher field gradients seen by the bunch for a constant power. However, due to the dispersive nature of the DLW, only frequency components with a phase velocity close to the beam velocity will remain synchronous with the beam over a long distance. From Figure 2a, one can see that the phase velocity is always higher than the group velocity, thus any beam synchronous beam will eventually overtake the pulse.

As previously mentioned, as the frequency changes, so does the distribution of field in the vacuum and dielectric regions. If we assume the total power in both regions is conserved, and that the normalised amplitudes of the fields in the electric and magnetic regions respectively are A and B, which are both proportional to $\sqrt{P_{in}}$ where P_{in} is the THz power flow into the structure, then $A^2+B^2 \propto P_{in}$, combining this with Eq. 4, we obtain

$$A \propto \left|\sqrt{\frac{r_{vd}^2 P_{in}}{r_{vd}^2+1}}\right|. \quad (5)$$

MODELLING THE FIELD FOR A BROADBAND PULSE

If we assume that an input THz pulse has amplitude $V(t) = \alpha\sqrt{P_{in}(t)}$, where α is a constant to allow us to modify the field amplitudes in the DLW. To obtain the THz amplitude at specific frequencies, we must take a Fourier transform of this input pulse

$$\mathcal{V}(\omega) = FT(V(t)). \quad (6)$$

where $FT(\ldots)$ is the Fourier transform operation. From Eq. 3 we know $\mathcal{E}(\omega,\ \beta_{mn})$ and $\mathcal{H}(\omega,\ \beta_{mn})$, where $\mathcal{E}$ and $\mathcal{H}$ are the E- and H-fields in the frequency domain. From the dispersion relation we can define β_{mn} as a function of ω. To account for the propagation of the pulse along the waveguide, we transform $e^{-j\beta_{mn}z}$ in Eq. 3 to $e^{-j\beta_{mn}(z+v_pt)}$, but $v_p = \omega/\beta_{mn}$, therefore we get $e^{-j(\beta_{mn}z+\omega t)}$. From the dispersion relation, we can again represent this as $e^{-j(\beta_{mn}(\omega)z+\omega t)}$ and when we integrate over all frequencies, this becomes a 'spatio-temporal' inverse Fourier transform [2] and we can now define the E- and H-fields in the time domain for a broadband pulse as

$$\begin{aligned}E(x,y,z,t) &= FT^{-1}\left(\left|\frac{r_{vd}(\omega)}{\sqrt{r_{vd}^2(\omega)+1}}\right|\mathcal{V}(\omega)\mathcal{E}(\omega)\right)\\ H(x,y,z,t) &= FT^{-1}\left(\left|\frac{r_{vd}(\omega)}{\sqrt{r_{vd}^2(\omega)+1}}\right|\mathcal{V}(\omega)\mathcal{H}(\omega)\right).\end{aligned} \quad (7)$$

Figure 3 shows the accelerating gradient on axis for a single-cycle initial pulse [3]. The figure shows the electric field for the pulse after it has propagated 1 mm into the structure and the inset figure shows when the pulse has traveled 1 μm into the structure, to show the pulse dispersion as it propagates through the structure. While we show this method for producing field maps for a broadband pulse in a rectangular DLW, this approach can be used for any broadband pulse, regardless of whether this is an accelerating mode, deflecting or any other mode.

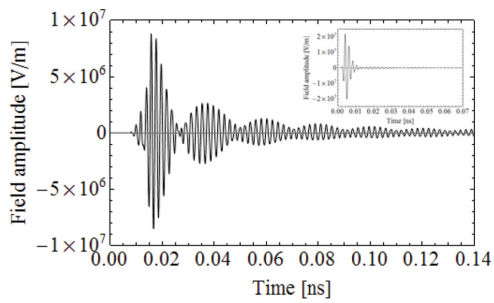

Figure 3: Field amplitude of a single-cycle pulse, 1 mm into the DLW. Inset is the pulse 1 μm into the DLW, showing the broadening due to loss of lower-frequency components [3].

ISBN: 978-3-95450-194-6 doi:10.18429/JACoW-LINAC2018-TUPO113

TRACKING SIMULATIONS

Conventional tracking codes, such as ASTRA, PARMELA, GPT and ELEGANT [4–7], import 1, 2 or 3D field maps, for the 1D case, Maxwell's equations are then used to expand the field map into 3D, and then the codes multiply the field map by $e^{-j\omega t+\phi_{RF}}$ and take the real part as the instantaneous field map. For broadband pulses, this approach does not work. Instead we need a 3D field map for each time step, hence a 4D field map.

Implementation

Initial tracking simulations to study the energy gain vs longitudinal position have been undertaken, looking at different pulse durations (Figure 4). Further details of the studies can be found in [3].

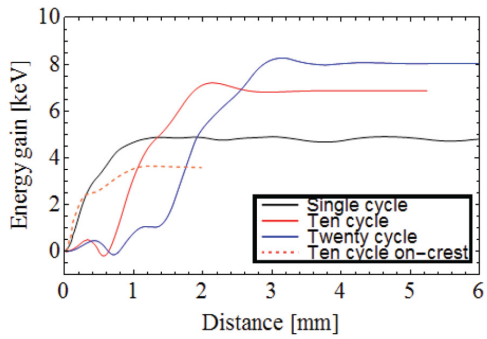

Figure 4: Energy gain vs longitudinal position in the DLW for different pulse durations [3].

Further to this, 6D particle tracking has been simulated using RF-Track [8] and also with a simple 4th-order Runge-Kutta integrator (RK4). The horizontal, vertical and longitudinal phase space distributions are shown respectively in Figures 5-7. The transverse distributions are collimated at ±200 μm, but there is no collimation after the DLW.

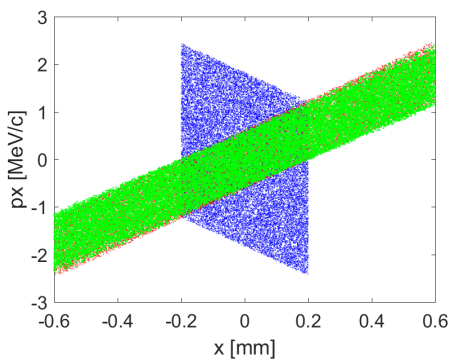

Figure 5: Horizontal phase space distribution before the DLW (blue) and after the DLW, tracked in RF-Track (red) and with an RK4 integrator (green).

The transverse phase space distributions agree well between RF-Track and the RK4 method, however the RK4 integrator exhibits a larger observed momentum spread in the longitudinal phase space distribution; particularly near the extremes of the sinusoidal modulation. Further studies are required to fully understand this.

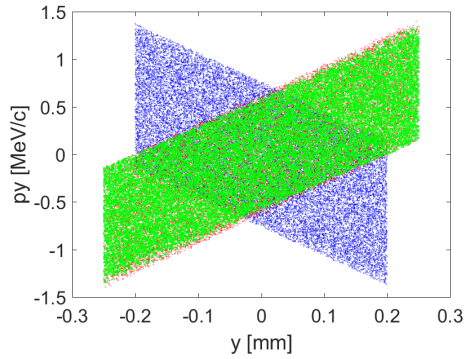

Figure 6: Vertical phase space distribution before the DLW (blue) and after the DLW, tracked in RF-Track (red) and with an RK4 integrator (green).

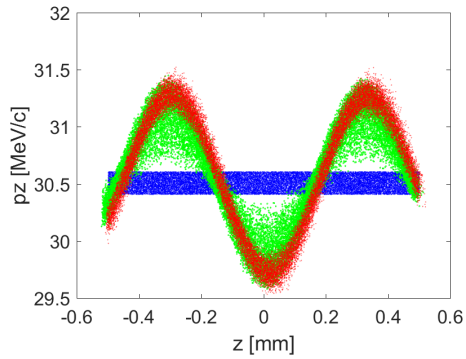

Figure 7: Longitudinal phase space distribution before the DLW (blue) and after the DLW, tracked in RF-Track (red) and with an RK4 integrator (green).

CONCLUSION

Conventional tracking codes assume single frequency fields and are therefore not suitable for modeling broadband pulses. We describe a method for producing field maps for broadband pulses which is completely general and can be applied to any structure and any mode. This method essentially extends the multiplication of a 3D field map by $e^{-j(\omega t+\phi_{RF})}$ to a Fourier transformation. We demonstrate this method for a rectangular dielectric lined waveguide (DLW) and show that the general field maps are 4D rather than 3D as used for single frequency tracking.

1D and 4D tracking simulations of broadband pulses have been presented. We perform 6D tracking simulations with a 4th-order Runge-Kutta (RK4) integrator and compare to RF-Track simulation results. A comparison of these results shows a good qualitative agreement, however there is some disagreement of the energy spread between the two methods. Further studies will be conducted to understand these disparities and to further develop a tracking technique to allow for more general tracking, such as including wakefields directly into the field maps.

ISBN: 978-3-95450-194-6 doi:10.18429/JACoW-LINAC2018-TUPO113

REFERENCES

[1] L. Xiao, W. Gai, X. Sun, "Field analysis of a dielectric-loaded rectangular waveguide accelerating structure", DOI: 10.1103/PhysRevE.65.016505.

[2] S. V. Samsonov, A. D. R. Phelps, V. L. Bratman, G. Burt, G. G. Denisov, A. W. Cross, K. Ronald, W. He and H. Yin, "Compression of Frequency-Modulated Pulses using Helically Corrugated Waveguides and its Potential for Generating Multigigawatt RF Radiation," DOI: 10.1103/PhysRevLett.92.118301.

[3] A. L. Healy, G. Burt, S. P. Jamison, "Group velocity matching in dielectric-lined waveguides and its role in electron-terahertz interaction," IPAC'17, Copenhagen, May 2017, WEPVA019, p. 3296

[4] A Space Charge Tracking Algorithm, http://www.desy.de/~mpyflo/

[5] The particle tracking code PARMELA, https://cds.cern.ch/record/749735

[6] General Particle Tracer, http://www.pulsar.nl/gpt/

[7] User manual for elegant, https://ops.aps.anl.gov/manuals/elegant_latest/elegant.html

[8] RF-Track: beam tracking in field maps including space-charge effects. Features and benchmarks, LINAC16, East Lansing, MI, USA, 2016 http://linac2016.vrws.de/papers/moprc016.pdf